

Constraints on radiatively inefficient accretion history from Eddington ratio distribution of active galactic nuclei

Xinwu Cao¹*, Ya-Di Xu²†

¹ Shanghai Astronomical Observatory, Chinese Academy of Sciences, 80 Nandan Road, Shanghai, 200030, China

² Physics Department, Shanghai Jiaotong University, 1954 Huashan Road, Shanghai, 200030, China

Accepted 2007 February 09

ABSTRACT

The transition of a standard thin disk to a radiatively inefficient accretion flow (RIAF) is expected to occur, when $\dot{m} \sim \dot{m}_{\text{crit}}$ ($\dot{m} = \dot{M}/\dot{M}_{\text{Edd}}$). The radiative efficiencies of accretion flows accreting at rates lower than the critical accretion rate \dot{m}_{crit} become significantly lower than that of standard thin disks. It is believed that the initial transition radius is small just after the accretion mode transition, and then the transition radius increases with decreasing accretion rate, as suggested by some theoretical models and observations. Based on such variable transition radius models, we derive how the accretion rate $\dot{m}(t)$ evolves with time from the observed Eddington ratio distribution for a sample of low-luminosity active galactic nuclei in the local universe. The derived time-dependent accretion rates $\dot{m}(t)$ show a rapid decrease after the transition of the standard thin accretion disk to a RIAF, which is consistent with that derived from the hard X-ray background.

Key words: galaxies: active—quasars: general—accretion, accretion disks—black hole physics

1 INTRODUCTION

Accretion onto massive black holes is believed to power active galactic nuclei (AGNs). The UV/optical continuum emission observed in luminous quasars is attributed to the thermal radiation from the accretion disks surrounding the massive black holes in quasars (e.g., Sun & Malkan 1989). In recent years, some different approaches are proposed to measure the masses of the central black holes in AGNs (e.g., Peterson 1993; Ferrarese & Merritt 2000; Gebhardt et al. 2000), and the central black hole masses of many AGNs can be measured fairly accurately. It is found that a fraction of luminous AGNs are accreting at extremely high rates. Their bolometric luminosities are around (or even higher than) the Eddington luminosity, for example, the black holes in many narrow-line Seyfert 1 galaxies are believed to be accreting at Eddington (or super-Eddington) rates (e.g., Sulentic et al. 2000; Warner et al. 2004; Bian & Zhao 2004; Chen & Wang 2004). Besides the luminous AGNs accreting at high Eddington rates ($\gtrsim 0.01$), many nearby low-luminosity AGNs are found to have similar characteristics as those luminous AGNs, but with relatively weaker broad-line emission and lower luminosities in different wavebands (Ho et al. 1997). Most of these low-luminosity AGNs are accreting at highly sub-Eddington rates ($L_{\text{bol}}/L_{\text{Edd}} \ll 0.01$). The Eddington ratios of AGNs can spread over more than ten orders of magni-

tude (from $\lesssim 10^{-10}$ to more than unity)(e.g., Wu & Cao 2005; Hopkins, Narayan & Hernquist 2006).

It is believed that standard thin disks (or slim disks) are present in luminous AGNs, while the radiatively inefficient accretion flows (RIAFs) are suggested to be present in those low-luminosity AGNs accreting at relatively low rates (Narayan & Yi 1994; Blandford & Begelman 1999, 2004; Igumenshchev, Abramowicz & Narayan 2000; Narayan, Igumenshchev & Abramowicz 2000). There is a critical accretion rate \dot{m}_{crit} , above which the RIAF is suppressed and a standard thin disk is present. The RIAF may connect to a standard thin disk at a certain transition radius R_{tr} . This is required by modelling on a variety of observations of AGNs (e.g., Quataert et al. 1999; Lu & Wang 2000; Cao 2003; Kong et al. 2004; Yuan, Quataert & Narayan 2004), and is also predicted by some theoretical model calculations (Abramowicz et al. 1995; Liu et al. 1999; Rozanska & Czerny 2000; Spruit & Deufel 2002). In all these models, the transition radius r_{tr} ($r_{\text{tr}} = R_{\text{tr}}/R_{\text{S}}$, and $R_{\text{S}} = GM_{\text{bh}}/c^2$) is expected to increase with decreasing accretion rate \dot{m} .

The evolution of central engines in AGNs is mainly governed by accretion processes. The black hole accretion processes are regulated by the gases supplied near the black hole, i.e., sufficient gases supplied probably lead to a high accretion rate, and vice versa (Springel, Di Matteo & Hernquist 2005; Di Matteo, Springel & Hernquist 2005; Hopkins, & Hernquist 2006). As the gases being swallowed by the black hole, the

* E-mail: cxw@shao.ac.cn

† E-mail: ydxu@sjtu.edu.cn

accretion rate decreases with time. An AGN will die off, while the gases near the black hole are finally exhausted. How the accretion rate \dot{m} evolves with time remains to be an open issue, though an exponentially time-dependent accretion rate $\dot{m}(t)$ was widely employed in many previous works (e.g., Park & Vishniac 1990; Haiman & Loeb 1998; Kauffmann & Haehnelt 2000). McMillan, Lightman & Cohn (1981) found accretion rate $\dot{m}(t) \propto t^{-2}$, if the gases accreted by the black hole are assumed to be supplied by stellar collisions or tidal disruptions in a dense star system surrounding the black hole. Compared with exponentially time-dependent accretion rate, this form of accretion rate changes very slowly with time. Many quasar evolution model calculations showed that the exponentially time-dependent quasar light curve (or simply a step function quasar light curve) can well reproduce the observed quasar luminosity functions (e.g., Haiman & Loeb 1998; Wyithe & Loeb 2002). Recently, the numerical simulations on the quasar activity triggered by the galaxy merger showed that the quasar accretion rate curve is very complicated (Springel, Di Matteo & Hernquist 2005; Di Matteo, Springel & Hernquist 2005). In their simulations, the gases near the black hole are blown away by the bright quasar radiation, and then accretion rate declines rapidly to switch off the quasar activity.

In principle, the evolution of the AGN light curve $L(t)$ can be derived from the Eddington ratio distribution of an AGN sample, because the Eddington ratio distribution $\xi[\log(L/L_{\text{Edd}})] \propto [\text{d} \log(L/L_{\text{Edd}})/\text{d}t]^{-1}$ (e.g., Begelman & Celotti 2004; Hopkins, Narayan & Hernquist 2006). However, it is still not straightforward to derive the time-dependent accretion rate $\dot{m}(t)$, because the radiative efficiency is no longer a constant when the accretion disk is evolving from slim disk (high- \dot{m}) (e.g., Abramowicz et al. 1988; Wang et al. 1999) to a RIAF (low- \dot{m}) (e.g., Narayan & Yi 1994).

In this work, we derive how the accretion rate $\dot{m}(t)$ evolves with time from an observed Eddington ratio distribution for a low-luminosity AGN sample in the local universe based on the standard disk/RIAF transition model. In our calculations, the physics of different accretion models and the accretion mode transition is properly considered.

2 SPECTRA OF RADIATIVELY INEFFICIENT ACCRETION FLOWS

The transition of a standard thin disk to a RIAF occurs, when the accretion rate \dot{m} decreases to a value below \dot{m}_{crit} . The structure of the RIAF is well described by the self-similar solution, except the region near the black hole (Narayan & Yi 1995; Yi 1996). The spectrum of a RIAF, $L_{\lambda}(M_{\text{bh}}, \dot{m}, \alpha, \beta)$, can be calculated approximately based on the self-similar solution (e.g., Mahadevan 1997; Chang, Choi & Yi 2002; Wu & Cao 2005), if the parameters M_{bh} , \dot{m} , α , and the fraction of the magnetic pressure β , are specified. However, the physical quantities of a self-similar RIAF deviate significantly from the global solution of the RIAF in its inner region, which may lead to inaccuracy for its spectral calculation, because most gravitational energy of the accreting matter is released in the inner region of the accretion flow.

In this work, we calculate the global structure of the accretion flows surrounding massive Schwarzschild black holes. The accretion flow is described by a set of general relativistic hydrodynamical equations (see Manmoto 2000, for the details). All the radiation processes are included in the calculations of the global accretion

flow structure. Integrating these equations from the outer boundary of the flow at $R = R_{\text{out}}$ inwards the black hole, we can obtain the global structure of the accretion flow passing the sonic point smoothly to the black hole horizon. In our calculations, the values of some parameters adopted are different from those in Manmoto (2000), which will be discussed in Section 7. We can then calculate the spectrum of the accretion flow based on this global structure of the RIAF. In the spectral calculations, the gravitational redshift effect is considered, while the relativistic optics near the black hole is neglected. We only calculate the total luminosity radiated from the RIAF without considering its inclination. The derived spectrum in this way can be taken as an average spectrum for AGNs, which is a good approximation, as AGNs should have randomly distributed orientations.

3 SPECTRA OF STANDARD DISKS

For a standard thin disk, the flux due to viscous dissipation in unit surface area is (Shakura & Sunyaev 1973)

$$F_{\text{vis}}(R) \simeq \frac{3GM_{\text{bh}}\dot{M}}{8\pi R^3} \left[1 - \left(\frac{3R_{\text{S}}}{R} \right)^{1/2} \right], \quad (1)$$

where $R_{\text{S}} = 2GM_{\text{bh}}/c^2$. The local disk temperature of the thin cold disk is

$$T_{\text{disk}}(R) = \frac{F_{\text{vis}}^{1/4}(R)}{\sigma_{\text{B}}^{1/4}}, \quad (2)$$

by assuming local blackbody emission. In order to calculate the disk spectrum, we include an empirical color correction for the disk thermal emission as a function of radius. The correction has the form (Chiang 2002)

$$f_{\text{col}}(T_{\text{disk}}) = f_{\infty} - \frac{(f_{\infty} - 1)[1 + \exp(-\nu_{\text{b}}/\Delta\nu)]}{1 + \exp[(\nu_{\text{p}} - \nu_{\text{b}})/\Delta\nu]}, \quad (3)$$

where $\nu_{\text{p}} \equiv 2.82k_{\text{B}}T_{\text{disk}}/h$ is the peak frequency of blackbody emission with temperature T_{disk} . This expression for f_{col} goes from unity at low temperatures to f_{∞} at high temperatures with a transition at $\nu_{\text{b}} \approx \nu_{\text{p}}$. Chiang (2002) found that $f_{\infty} = 2.3$ and $\nu_{\text{b}} = \Delta\nu = 5 \times 10^{15}$ Hz can well reproduce the model disk spectra of Hubeny et al. (2001). The disk spectra can therefore be calculated by

$$L_{\nu} = 32\pi^2 \left(\frac{GM_{\text{bh}}}{c^2} \right)^2 \frac{h\nu^3}{c^2} \int_{r_{\text{in}}}^{\infty} \frac{rdr}{f_{\text{col}}[\exp(h\nu/f_{\text{col}}k_{\text{B}}T_{\text{disk}}) - 1]}, \quad (4)$$

where $r_{\text{in}} = R_{\text{in}}/R_{\text{S}}$ is the inner radius of the standard disk. At a high accretion rate, $\dot{m} > \dot{m}_{\text{crit}}$, the standard thin disk extends to the minimum stable orbit of the black hole, $r_{\text{in}} = 3$, for a non-rotating black hole. For a RIAF+standard thin disk system, the spectrum emitted from the standard disk region can be calculated by using the transition radius r_{tr} ($r_{\text{tr}} = R_{\text{tr}}/R_{\text{S}}$) instead of r_{in} as the lower integral limit in Eq. (4).

4 TRANSITION RADIUS R_{tr} BETWEEN RIAF AND STANDARD THIN DISK

In this work, we assume the transition from a standard thin disk to a RIAF to occur whenever $\dot{m} \lesssim \dot{m}_{\text{crit}}$, i.e., so-called "strong principle" (e.g., Narayan, Mahadevan & Quataert 1998). The RIAF is naturally expected to match a standard thin disk at the transition

radius r_{tr} . The detailed physics, causing such a transition of a standard thin disk to a RIAF, is still unclear. It is suggested that the standard thin disk transits are truncated at an initial transition radius $r_{\text{tr},0}$ and a RIAF is present within this radius, when $\dot{m} = \dot{m}_{\text{crit}}$. The transition radius r_{tr} increases with decreasing accretion rate \dot{m} as

$$r_{\text{tr}} \propto \dot{m}^{-p}, \quad (5)$$

where $p = 2$ is predicted, based on the scenario of transition triggered by the thermal instability, by Abramowicz et al. (1995); or $p \simeq 0.8 - 1.3$ is expected by the disk evaporation induced transition scenarios (Liu et al. 1999; Rozanska & Czerny 2000; Spruit & Deufel 2002). In either one of these transition scenarios, the transition radius r_{tr} always increases with decreasing accretion rate \dot{m} . The precise initial transition radius $r_{\text{tr},0}$ is still unknown, though it should be small. In this work, we adopt $r_{\text{tr},0} = 20$ in all our calculations.

5 THE OBSERVED DISTRIBUTION OF THE EDDINGTON RATIO L_B/L_{Edd}

In this work, we adopt the sample given by Ho (2002), in which 74 nearby supermassive black holes with both measured masses and B-band luminosities. The black hole masses of the sources in this sample have been measured by using two different approaches: stellar and gas kinematics and reverberation mapping. Terashima, Ho & Ptak (2000) found that X-ray luminosities in 2–10 keV of LINERs (low-ionization nuclear emission-line regions) with broad H α emission in their optical spectra are proportional to their H α luminosities. This indicates that the dominant ionizing source in LINERs is photoionization by hard photons from low-luminosity AGNs. The B-band luminosities of the sources in this sample are estimated from the line emissions, which are supposed to be photo-ionized by the nuclear radiations. This may cause some uncertainties for individual sources, but the derived Eddington ratio should still be reliable in statistical sense. This sample includes 17 PG quasars, which may not be in the same population with those low-luminosity counterparts and are accreting at higher rates $\dot{m} > \dot{m}_{\text{crit}}$. As we are focusing on the inefficient accretion history of AGNs, we leave out these 17 PG quasars, which leads to 57 sources. The Eddington ratio distribution for this sample is plotted in Fig. 1. This sample was used to explore the evolution of low-luminosity AGNs by Hopkins, Narayan & Hernquist (2006). The selection effects of this sample were extensively analyzed in their work (see Section 2.1 in their paper for the details). They found that, the FR I radio galaxies from the sample used by Marchesini, Celotti & Ferrarese (2004) exhibit significant different luminosity distribution from that of the sample by Ho (2002), while both of these two sample exhibit similar Eddington ratio distributions. This means that the results of AGN evolution derived from either one of these two samples would be qualitatively unchanged, which may imply that the derived results are not affected significantly by selection effects.

The maximal distance for the sources measured by reverberation mapping method is about 3 times that of the subsample measured by the stellar/gas kinematics. Hopkins, Narayan & Hernquist (2006) suggested to multiply the relative fraction of the sources measured kinematics by 3^3 to account for the different subsample volumes. The derived distribution for this tentatively volume-corrected sample is also plotted in Fig. 1.

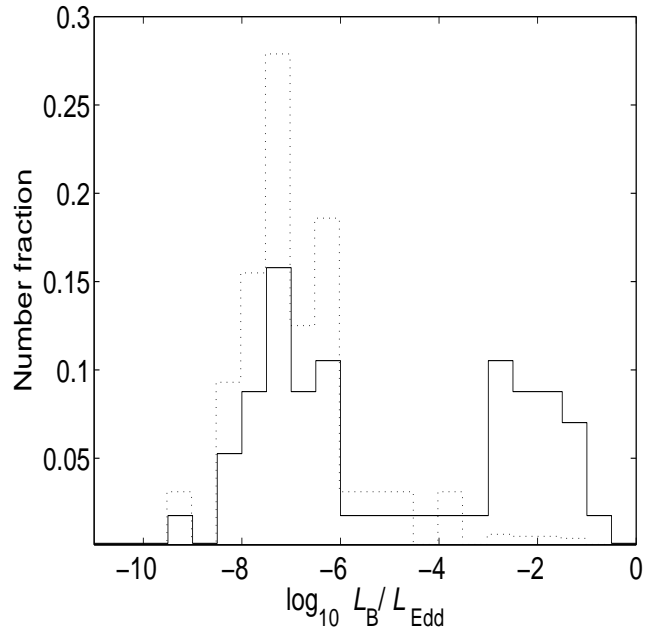


Figure 1. The distribution of the Eddington ratio L_B/L_{Edd} at B-band for the sample given by Ho (2002) (the solid line). The dotted line is the distribution for the effective volume-corrected sample (see Section 5 for the details).

6 THE TIME-DEPENDENT ACCRETION RATE $\dot{m}(t)$ DERIVED FROM THE EDDINGTON RATIO DISTRIBUTION

The light curve of AGNs at B-band can be derived from the observed Eddington ratio distribution $dN/d\log(L_B/L_{\text{Edd}})$:

$$\frac{d\log(L_B/L_{\text{Edd}})}{dt} = N^{\text{tot}} \left(\frac{dN}{d\log(L_B/L_{\text{Edd}})} \right)^{-1}, \quad (6)$$

where N^{tot} is the total number of the sources in the sample, and t is normalized to unity. The time-dependent accretion rate $\dot{m}(t)$ can be derived from the light curve by

$$\frac{d\dot{m}(t)}{dt} = \frac{d\log(L_B/L_{\text{Edd}})}{dt} \left(\frac{d\log(L_B/L_{\text{Edd}})}{d\dot{m}} \right)^{-1}, \quad (7)$$

where $d\log(L_B/L_{\text{Edd}})/d\dot{m}$ is available based on spectral calculations for the accretion mode transition model described in Sections 2–4. Here, we have to assume that all sources have the same time-dependent accretion rate $\dot{m}(t)$, and it evolves monotonically with time. The latter assumption may not be the case for some individual sources in short timescales, but it should be reasonable in statistic sense for a sample of AGNs, because accretion rates should decline in a long timescale. Substituting Eq. (6) into Eq. (7), we obtain

$$\frac{d\dot{m}(t)}{dt} = N^{\text{tot}} \left(\frac{dN}{d\dot{m}} \right)^{-1}. \quad (8)$$

Using the X-ray luminosity function of AGNs given by Ueda et al. (2003), we calculate number density of AGNs in comoving space as a function of redshift. It is found that the number density of AGNs in the local universe is about 45 per cent of that at $z = 0.5$, which implies that the AGNs at low redshifts are roughly in a steady evolving state with switching on and off being in balance. The cosmological evolution of AGNs at low redshifts should be unimpor-

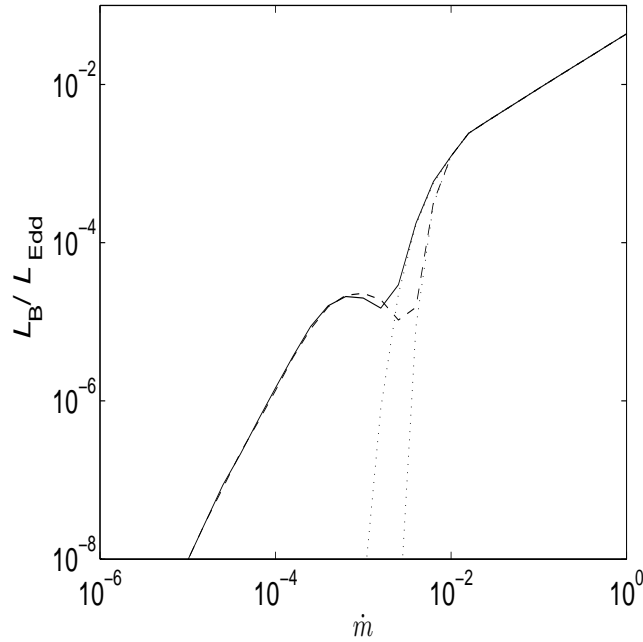


Figure 2. The spectral evolution of RIAF+standard thin disk systems with varying transition radii r_{tr} . The dotted lines represent the emission from the outer standard thin disk regions. The solid line represents the case for $p = 1$, while the dashed line is for $p = 2$.

tant, which will affect our results very little, as the sample used in this work is limited to the sources in the local universe.

7 RESULTS

The detailed physics of the viscosity in accretion disks is still quite unclear, and it is usually described by the viscosity parameter α . Assuming accretion to be driven by turbulent stresses generated by the magnetorotational instability, the three-dimensional MHD simulations suggest that the viscosity parameter α in the accretion flows is ~ 0.1 (Armitage 1998), or $\sim 0.05 - 0.2$ (Hawley & Balbus 2002). The critical accretion rate $\dot{m}_{\text{crit}} \simeq 0.01$ for accretion mode transition is suggested by different authors either from observations or theoretical arguments (see, e.g., Narayan, Mahadevan & Quataert 1998). Our numerical calculations for the global structure of the flows show $\dot{m}_{\text{crit}} \simeq 0.01$ for $\alpha = 0.2$. In this work, we adopt the α -viscosity, $\alpha = 0.2$, and limit our calculations of the RIAF structure to hydrodynamics, but the magnetic pressure is included by a parameter β . The parameter β , defined as $p_m = (1 - \beta)p_{\text{tot}}$, describes the magnetic field strength of the gases in the flow. This parameter is in fact not a free parameter, which is related to the viscosity parameter α as $\beta \simeq (6\alpha - 3)/(4\alpha - 3)$, as suggested by the MHD simulations (Hawley, Gammie & Balbus 1996; Narayan, Mahadevan & Quataert 1998). For $\alpha = 0.2$, $\beta \simeq 0.8$ is required. Manmoto (2000) adopted very small values of δ in the calculations, as those of traditional advection dominated accretion flow (ADAF) models (see Narayan 2002, for a review, and references therein). It was pointed out that such a small δ adopted in traditional ADAF models is very unlikely, because a significant fraction of the viscously dissipated energy (up to $\delta \sim 0.5$) could go into electrons by magnetic reconnection, if the magnetic fields in the flow are strong (Bisnovatyi-Kogan & Lovelace 1997,

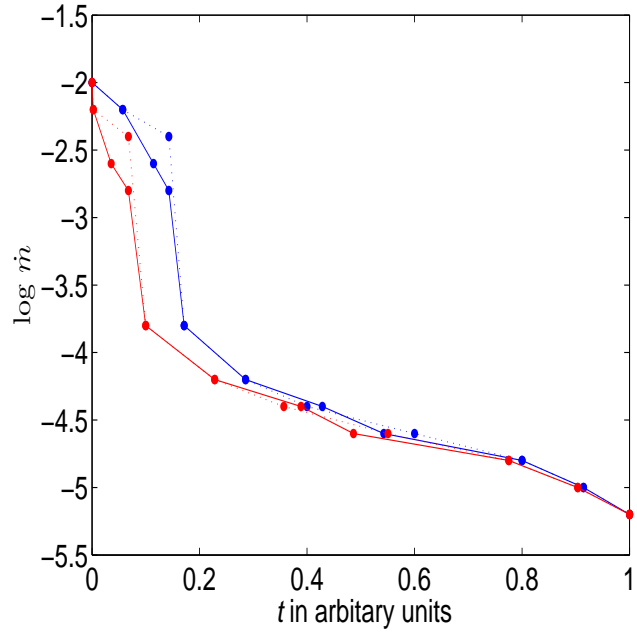


Figure 3. The derived time-dependent accretion rates $\dot{m}(t)$. The blue lines represent the cases derived directly from Ho (2002)'s sample, while the red lines are for the effective volume-corrected sample. The solid lines are for the cases of $p = 1$, while the dotted lines are for $p = 2$.

2000). The average black hole mass for the sources in this sample is $\simeq 2.4 \times 10^8 M_{\odot}$. In our calculations, we adopt $\delta = 0.5$, and $M_{\text{bh}} = 2.4 \times 10^8 M_{\odot}$. Our numerical calculations show that the dimensionless light curves L_B/L_{Edd} as function of \dot{m} change very little for different black hole masses adopted (in the range of $\sim 10^{6-10} M_{\odot}$).

Using the method described in Sections 2 and 3, we can calculate the global accretion flow structure and then the spectrum varying with accretion rate \dot{m} and r_{tr} . The initial transition radius $r_{\text{tr},0} = 20$ is adopted in all our calculations for RIAFs. The Eddington ratios L_B/L_{Edd} evolving with \dot{m} are plotted in Fig. 2. The time-dependent accretion rates $\dot{m}(t)$ can be derived from the observed Eddington ratio distributions by using Eqs. (6) and (7) (see Fig. 3).

8 DISCUSSION

For a RIAF+standard thin disk system, its optical emission is mostly from the outer thin accretion disk region, if its accretion rate \dot{m} is close to the critical value \dot{m}_{crit} , because the transition radius is small for this case. For a large transition radius, corresponding to a low \dot{m} , the temperature of the standard thin disk region is very low, and the optical emission is dominantly from the inner RIAF (see Fig. 2). The optical luminosity drops rapidly with \dot{m} , when the flow is accreting at $\lesssim \dot{m}_{\text{crit}}$.

In Fig. 2, we find that the luminosity decreases rapidly after the accretion mode transition at $\dot{m} = \dot{m}_{\text{crit}} \sim 0.01$. It is found that the light curves $L_B(\dot{m})$ are almost same for $p = 1$ and $p = 2$, except the accretion rate \dot{m} is in the range of $\sim 0.004 - 0.01$. When the accretion rate \dot{m} is slightly lower than \dot{m}_{crit} , the emission is dominantly from the outer thin disk regions, because the standard thin disks still extend to small radii. The emission becomes dom-

inated by the radiation from the inner RIAFs, when the accretion rate $\dot{m} \lesssim 5 \times 10^{-3}$.

Based on the relations between accretion rate \dot{m} and B-band luminosity $L_B(\dot{m})$ given in Fig. 2, we can derive the time-dependent accretion rates $\dot{m}(t)$ from the observed Eddington ratio distributions for AGNs. In Fig. 3, we plot the derived $\dot{m}(t)$ for the cases with two different values of p for variable transition radius models, from the Eddington ratio distribution of the Ho (2002)'s sample or the sample with effective volume-corrected (see Section 5), respectively. We find that there is a rapid decrease of $\dot{m}(t)$ from 10^{-2} to $\sim 10^{-4}$ either for the cases with different values of p or from different Eddington ratio distributions (the original one or the effective volume-corrected one). It is not surprised to find that the derived time-dependent accretion rates $\dot{m}(t)$ are quite similar for the cases with $p = 1$ or $p = 2$, because the theoretical curves $L_B(\dot{m})$ are very similar for these two different values of p (see Fig. 2). For the Eddington ratio distribution of the effective volume-corrected sample, there are more sources with low luminosities, i.e., less sources with \dot{m} close to \dot{m}_{crit} , so the derived time-dependent $\dot{m}(t)$ decreases more rapidly than that derived from the original sample. We find that the main feature of the time-dependent $\dot{m}(t)$ has not been changed by this effective volume-corrected sample. Cao (2005) calculated the hard X-ray emission from all RIAFs in faint AGNs, and compared them with the observed X-ray background. It was found that the accretion rate should decrease rapidly to the value far below the critical rate within a timescale shorter than 5 per cent of bright quasars' lifetime, which is consistent with our present time-dependent accretion rates $\dot{m}(t)$ derived from the Eddington ratio distributions. The present derived time-dependent $\dot{m}(t)$ is based on the assumption of monotonical evolution with time. From Eq. (8), we find that $d\dot{m}(t)/dt$ also represents the distribution of accretion rates \dot{m} for the sample.

The present sample may have overlooked a number of sources with very low Eddington ratios ($\lesssim 10^{-5} - 10^{-6}$), which means a complete sample should include more sources accreting at very low rates $\lesssim 10^{-4}$ than the present sample. This implies that the relative timescale of the rapid drop of accretion rate from 0.01 to $\sim 10^{-4}$ should be even shorter than those plotted in Fig. 3, if a complete sample is adopted. Such a complete sample is still unavailable now, however, the main feature of $\dot{m}(t)$ with a rapid declining between 0.01 and $\sim 10^{-4}$ derived in this work will not be changed qualitatively.

The fraction of the viscously dissipated energy that directly goes into electrons, $\delta = 0.5$, is adopted in this work, as suggested by Bisnovatyi-Kogan & Lovelace (1997). The precise value of δ is still unknown, and it may slightly be lower than 0.5. If a slightly lower δ is adopted, the derived light curves $L_B(\dot{m})$ have the similar form, but they should be systematically lower than those in Fig. 2. Thus, the main feature of $\dot{m}(t)$, a rapid decrease after the accretion mode transition, will still be present as those plotted in Fig. 3.

The RIAF may have winds, and a power-law r -dependent accretion rate is assumed, though the detailed physics is still unclear (Blandford & Begelman 1999). When the accretion rate \dot{m} is close to 0.01, the optical emission is dominated by that from the outer standard thin disk region (see Fig. 2). Thus, the optical spectrum of the RIAF+standard thin disk system will not be affected by the winds of the RIAF, when \dot{m} is close to 0.01. The optical emission from the RIAFs is attributed to Compton up-scatterings of the soft synchrotron photons by the hot electrons in the accretion flows. Our numerical calculations on the RIAF spectra show that most optical emission (more than 90 per cent) is from the regions within $10 R_S$. This implies that the optical emission of a RIAF is similar to a

RIAFAF with winds, provided they have the same accretion rate at their inner edge. In this work, we focus on the accretion rate at the inner edge of the accretion flow, i.e., the mass of gases swallowed by the black hole. Thus, the derived time-dependent accretion rates at the inner edges of the RIAFs will not be altered much, even if winds are present in the RIAFs.

In all our calculations, the initial transition radius $r_{\text{tr},0} = 20$ is adopted. As the transition radius r_{tr} increases rapidly with decreasing accretion rate \dot{m} (see Eq. 5), the resulted light curves $L_B(\dot{m})$ will only be slightly different for different values of $r_{\text{tr},0}$ adopted, provided $r_{\text{tr},0}$ is not very large. Thus, the derived $\dot{m}(t)$ is insensitive to the value of $r_{\text{tr},0}$.

In principle, one has to consider the activity trigger rates of galaxies along the cosmic time in the study of AGN evolution. However, it is difficult to have a complete sample including both bright and faint AGNs, which can be used to explore the evolution of bright quasars to faint AGNs. In this work, we only explore the time-dependent $\dot{m}(t)$ for $\dot{m} \lesssim \dot{m}_{\text{crit}}$, and the sources in the sample we used are limited in the local universe. Thus, the results may not be affected by the unknown trigger rates, though it is unclear if the derived $\dot{m}(t)$ in this work is valid for the AGNs at high redshifts.

ACKNOWLEDGMENTS

We thank A. Loeb for the explanation on their quasar evolution models, R. Narayan for helpful conversation, and the anonymous referees for their comments and suggestions. This work is supported by the National Science Fund for Distinguished Young Scholars (grant 10325314), and NSFC (grant 10333020).

REFERENCES

- Abramowicz M. A., Chen X., Kato S., Lasota J. -P., Regev O., 1995, ApJ, 438, L37
- Abramowicz M. A., Czerny B., Lasota J. P., Szuszkiewicz E., 1988, ApJ, 332, 646
- Armitage P.J., 1998, ApJ, 501, L189
- Begelman M. C., Celotti A., 2004, MNRAS, 352, L45
- Bian W., Zhao Y., 2004, MNRAS, 352, 823
- Bisnovatyi-Kogan G. S., Lovelace R. V. E., 1997, ApJ, 486, L43
- Bisnovatyi-Kogan G. S., Lovelace R. V. E., 2000, ApJ, 529, 978
- Blandford R. D., & Begelman M. C., 1999, MNRAS, 303, L1
- Blandford R. D., & Begelman M. C., 2004, MNRAS, 349, 68
- Cao X., 2003, ApJ, 599, 147
- Cao X., 2005, ApJ, 631, L101
- Chang H.Y., Choi C.S., Yi I., 2002, AJ, 124, 1948
- Chen, L.-H., & Wang, J.-M., 2004, ApJ, 614, 101
- Chiang J., 2002, ApJ, 572, 79
- Di Matteo T., Springel V., Hernquist L., 2005, Nature, 433, 604
- Ferrarese L., Merritt D., 2000, ApJ, 539, L9
- Gebhardt K. et al., 2000, ApJ, 539, L13
- Haiman Z., Loeb A., 1998, ApJ, 503, 505
- Hawley J.F., Balbus S.A., 2002, ApJ, 573, 738
- Hawley J.F., Gammie C.F., Balbus, S.A., 1996, ApJ, 464, 690
- Ho, L. C., 2002, ApJ, 564, 120
- Ho L. C., Filippenko A. V., Sargent W. L. W., Peng, C. Y., 1997, ApJS, 112, 391
- Hopkins P. F., Hernquist L., 2006, ApJS, 166, 1
- Hopkins P.F., Narayan R., Hernquist L., 2006, ApJ, 643, 641
- Hubeny I., Blaes O., Krolik J. H., Agol E., ApJ, 559, 680

Igumenshchev I. V., Abramowicz M. A., Narayan R., 2000, *ApJ*, 537, L27

Kauffmann G., Haehnelt M., 2000, *MNRAS*, 311, 576

Kong M.Z., Wu X. -B., Han J. L., & Mao Y. F., 2004, *ChJAA*, 4, 518

Liu B. F., Yuan W., Meyer F., Meyer-Hofmeister E., Xie G. Z., 1999, *ApJ*, 527, L17

Lu Y., Wang T., 2000, *ApJ*, 537, L103

Mahadevan R., 1997, *ApJ*, 477, 585

Manmoto T., 2000, *ApJ*, 534, 734

Marchesini D., Celotti A., & Ferrarese L., 2004, *MNRAS*, 351, 733

McMillan S.L.W., Lightman A.P., Cohn H., 1981, *ApJ*, 251, 436

Narayan R., 2002, in *Lighthouses of the Universe: The Most Luminous Celestial Objects and Their Use for Cosmology Proceedings of the MPA/ESO/*, p. 405

Narayan R., Igumenshchev I. V., Abramowicz M. A., 2000, *ApJ*, 539, 798

Narayan R., Mahadevan R., Quataert, E., 1998, in *Theory of Black Hole Accretion Disks*, edited by Marek A. Abramowicz, Gunnlaugur Bjornsson, and James E. Pringle. Cambridge University Press, 1998., p.148

Narayan R., Yi I., 1994, *ApJ*, 428, L13

Narayan R., Yi I., 1995, *ApJ*, 452, 710

Narayan R., Yi I., Mahadevan R., 1995, *Nature*, 374, 623

Park S.J., Vishniac E.T., 1990, *ApJ*, 353, 103

Peterson B. M., 1993, *PASP*, 105, 247

Quataert E., Di Matteo T., Narayan R., Ho L. C., 1999, *ApJ*, 525, L89

Rozanska A., Czerny B., 2000, *A&A*, 360, 1170

Shakura N. I., Sunyaev R. A., 1973, *A&A*, 24, 337

Springel V., Di Matteo T., Hernquist L., 2005, *MNRAS*, 361, 776

Spruit H. C., Deufel B., 2002, *A&A*, 387, 918

Sulentic J. W., Zwitter T., Marziani P., Dultzin-Hacyan D., 2000, *ApJ*, 536, L5

Sun W. -H., Malkan M. A., 1989, *ApJ*, 346, 68

Terashima Y., Ho L. C., Ptak A. F., 2000, *ApJ*, 539, 161

Ueda Y., Akiyama M., Ohta K., Miyaji T., 2003, *ApJ*, 598, 886

Wang J.-M., Szuszkiewicz E., Lu F.-J., Zhou Y.-Y., 1999, *ApJ*, 522, 839

Warner C., Hamann F., Dietrich M., 2004, *ApJ*, 608, 136

Wu Q., Cao X., 2005, *ApJ*, 621, 130

Wyithe J.S.B., Loeb A., 2002, *ApJ*, 581, 886

Yi I., 1996, *ApJ*, 473, 645

Yuan F., Quataert E., Narayan R., 2004, *ApJ*, 606, 894